

# Effect of Arterial Deprivation on Growing Femoral Epiphysis: Quantitative Magnetic Resonance Imaging Using a Piglet Model

Jung-Eun Cheon, MD<sup>1</sup>, Won Joon Yoo, MD<sup>2</sup>, In-One Kim, MD<sup>1</sup>, Woo Sun Kim, MD<sup>1</sup>, Young Hun Choi, MD<sup>1</sup>

<sup>1</sup>Department of Radiology, Seoul National University College of Medicine, and Institute of Radiation Medicine, SNUMRC, Seoul 110-744, Korea;  
<sup>2</sup>Department of Orthopedic Surgery, Seoul National University College of Medicine, Seoul 110-744, Korea

**Objective:** To investigate the usefulness of dynamic contrast-enhanced magnetic resonance imaging (DCE-MRI) and diffusion MRI for the evaluation of femoral head ischemia.

**Materials and Methods:** Unilateral femoral head ischemia was induced by selective embolization of the medial circumflex femoral artery in 10 piglets. All MRIs were performed immediately (1 hour) and after embolization (1, 2, and 4 weeks). Apparent diffusion coefficients (ADCs) were calculated for the femoral head. The estimated pharmacokinetic parameters (Kep and Ve from two-compartment model) and semi-quantitative parameters including peak enhancement, time-to-peak (TTP), and contrast washout were evaluated.

**Results:** The epiphyseal ADC values of the ischemic hip decreased immediately (1 hour) after embolization. However, they increased rapidly at 1 week after embolization and remained elevated until 4 weeks after embolization. Perfusion MRI of ischemic hips showed decreased epiphyseal perfusion with decreased Kep immediately after embolization. Signal intensity-time curves showed delayed TTP with limited contrast washout immediately post-embolization. At 1–2 weeks after embolization, spontaneous reperfusion was observed in ischemic epiphyses. The change of ADC ( $p = 0.043$ ) and Kep ( $p = 0.043$ ) were significantly different between immediate (1 hour) after embolization and 1 week post-embolization.

**Conclusion:** Diffusion MRI and pharmacokinetic model obtained from the DCE-MRI are useful in depicting early changes of perfusion and tissue damage using the model of femoral head ischemia in skeletally immature piglets.

**Index terms:** Diffusion-weighted imaging; Dynamic contrast enhanced MRI; Femoral head ischemia

## INTRODUCTION

It is generally accepted that disruption of blood supply

Received November 7, 2014; accepted after revision February 17, 2015.

This study was supported by research funds of Seoul National University Hospital (04-2007-0990).

**Corresponding author:** Won Joon Yoo, MD, Department of Orthopedic Surgery, Seoul National University Children's Hospital, 101 Daehak-ro, Jongno-gu, Seoul 110-744, Korea.

- Tel: (822) 2072-1966 • Fax: (822) 745-3367
- E-mail: yoowj@snu.ac.kr

This is an Open Access article distributed under the terms of the Creative Commons Attribution Non-Commercial License (<http://creativecommons.org/licenses/by-nc/3.0>) which permits unrestricted non-commercial use, distribution, and reproduction in any medium, provided the original work is properly cited.

to the growing femoral head is a key pathogenetic mechanism of Legg-Calvé-Perthes disease (LCPD) (1, 2). Experimental deprivation of blood circulation by methods such as femoral neck ligation, arterial deprivation, venous drainage obliteration, or manipulation with hyper-abduction of the hip in skeletally immature animals could duplicate pathologic findings indicative of LCPD in children (3–5). A piglet model of hip ischemia is a well-established animal model of osteonecrosis because the hip anatomy of piglets is similar to that of humans. Histopathologic and radiographic changes using the piglet model have been shown to resemble those observed in human LCPD (4, 6, 7).

Skeletal ischemia of the proximal femur has been primarily evaluated by observing established sequelae of osteonecrosis such as epiphyseal collapse and deformation

of the femoral head on plain radiographs. Early ischemic changes in the bone marrow can be demonstrated by abnormal signal change in magnetic resonance imaging (MRI) and abnormal uptake in bone scintigraphy (8). Several experimental studies demonstrated that diffusion MRI could be used as a biomarker of ischemic necrosis of the immature femoral head because water is organized around macromolecules. Tissue disorganization caused by ischemic injury would likely affect water diffusion (9, 10). Gadolinium-enhanced MRI has been used to demonstrate a lack of adequate blood flow in the femoral head in LCPD patients (11, 12). Dynamic contrast enhanced (DCE)-MRI has been utilized to extract kinetic parameters of bone perfusion. DCE-MRI was initially employed to depict tumor microvascularization (13-15). Its utility was then expanded to assess non-tumoral pathologies including synovial inflammatory diseases (16) and osteoporosis (17). Recently, peripheral bone microcirculation in the proximal femur has been studied with a focus on ischemic bone pathology (18, 19).

We hypothesized that arterial occlusion could cause LCPD-like pathologic changes in the femoral head. In addition, diffusion MRI and DCE-MRI could provide quantitative data related to tissue diffusion and microcirculation, thus allowing the monitoring of tissue ischemia and the perfusion-reperfusion status of the femoral head. The purpose of this study was to determine if diffusion MRI and DCE-MRI can depict early changes of perfusion and tissue damage in a model of femoral head ischemia induced by occlusion of the medial femoral circumflex artery in

skeletally immature piglets.

## MATERIALS AND METHODS

### Animal Model

The experiment protocol was approved by the Institutional Animal Care and Use Committee of our institution. Piglets (n = 10) were 3-5 weeks old with weight of 5-8 kg at the start of the intervention. Thus, the skeletal maturity of them corresponded to that of a 3 to 5 years old child. Ischemia was induced by disrupting the arterial supply of the femoral epiphysis using an arterial embolization technique. Anesthesia was introduced through an intramuscular injection of 50 mg of ketamine hydrochloride (Ketalar; Yuhanyanghang, Seoul, Korea) and 20 mg of xylazine hydrochloride (Rompun; Bayer Korea, Seoul, Korea) at 0.5 mL per kilogram of the body weight. After induction of anesthesia, a 4-French (Fr) femoral arterial sheath was placed at the common femoral artery using Seldinger technique. With the use of the 4-Fr catheter, contrast medium was injected using a power injector at a rate of 1.5 mL/s. Digital subtraction angiography was performed. After confirming normal arterial anatomy (Fig. 1A), a 2.4-Fr tip microcatheter (Microferret; Cook, Bloomington, IN, USA) was advanced into the medial circumflex femoral artery of the contralateral lower limb. N-butyl-2-cyanoacrylate (NBCA) (Histoacryl; B. Braun, Melsungen, Germany) was used as an embolic agent. Prior to injection of the NBCA mixture, the microcatheter was flushed with a 5% dextrose solution to



**Fig. 1. Occlusion of medial circumflex femoral artery.**

**A.** Aortography at level of bifurcation demonstrating angiographic anatomy of iliac and femoral arteries. Note medial circumflex femoral artery (arrow). **B.** Follow-up aortography demonstrating abrupt cutoff of medial circumflex femoral artery (arrow) suggesting successful embolization.

prevent premature polymerization of the mixture within the microcatheter. The NBCA mixture was injected using a 1-mL syringe under fluoroscopic monitoring. Post-embolization angiography was performed to confirm total occlusion of the arterial flow (Fig. 1B).

### MR Imaging

MR imaging was performed at 3 T (Signa Expert, GE Medical Systems, Milwaukee, WI, USA) by using a pair of 3-inch receive-only surface coils at approximately 1 hour and 1, 2, 4 weeks after surgery. Axial T1-weighted spin echo images were obtained with a 20-cm field of view (FOV), 256 x 256 matrix, 2.5-mm slice thickness, a 500 ms repetition time (TR), and a 9 ms echo time (TE). Fast spin echo T2-weighted images were acquired with TR/TE of 2000/60 msec. Diffusion-weighted imaging (DWI) was performed using a b-value of 700 mm<sup>2</sup>/s. Four signals of 4-mm section thickness and 1.25-mm in-plane resolution were acquired. DCE-MRI was obtained after manual injection of 0.1 mmol/kg of gadopentetate dimeglumine (Magnevist; Berlex, Wayne, NJ, USA) into an ear vein. Detailed imaging parameters for DCE-MR perfusion imaging were as follows: TR/TE at 5.4/1.3 msec; flip angle at 15°; FOV of 16 cm; matrix of 200 x 200. Dynamic perfusion imaging was acquired every 55 seconds for a total acquisition time of 4 minutes 35 seconds. DCE-MRI was performed using the same section orientations as used for conventional MR imaging to cover both hip joints. After dynamic contrast enhanced study, post-contrast spin echo T1-weighted images (TR/TE, 500/9 msec) were also obtained.

### MR Imaging Analysis

Dynamic contrast-enhanced magnetic resonance images were processed using the MR perfusion analysis method (nordicICE; Nordic Neuro Lab, Bergen, Norway), in which T1-weighted image was used for structural imaging. On the basis of 2-compartment pharmacokinetic model proposed by Brix, we used perfusion analysis method to calculate pharmacokinetic parameters. Pharmacokinetic modeling has been designed to offer information on the permeability between intravascular extracellular space and extravascular extracellular space (EES), extraction rate between EES and vessels,  $K_{ep}$  (mL·min<sup>-1</sup>·100 mL<sup>-1</sup>), and EES volume fraction  $V_e$  (%). In addition, semi-quantitative parameters based on concentration-time curves such as peak enhancement (PE), time to peak (TTP), and wash-out ( $Wash_{out}$ ) parameters were evaluated in femoral epiphysis. One pediatric radiologist

manually defined the regions of interest (ROI) on the secondary ossification center of the femoral epiphysis. Perfusion parameters were extracted from the ROI. Signal intensities from all voxels within the ROI were averaged to generate a single time intensity curve characteristic of the regions. Apparent diffusion coefficient (ADC) was also calculated from the ADC map by free-hand drawing of the ROI on the secondary ossification center in the femoral epiphysis. The ADC value was presented as the average ADC value of the ROI.

### Radiographic and Histologic Assessments

Animals were sacrificed arbitrarily at 1 week (n = 3), 2 weeks (n = 4), and 4 weeks (n = 3) following the induction of ischemic necrosis. The proximal part of the femur was dissected, examined visually, and radiographed as a whole using the Faxitron Cabinet X-ray System (Hewlett-Packard, McMinnville, OR, USA). The specimen was then fixed in 10% neutral buffered formalin for 2 weeks. Bones were subsequently decalcified in 25% formic acid until soft. The ends of bones were cut with a razor in the mid-coronal plane, photographed, and cut into smaller pieces to assess specific regions for structural changes. A pathologist evaluated the histopathological findings of the proximal femur by mainly focusing on the presence of osteonecrosis of the femoral epiphysis and cellular changes of the adjacent growth plate.

### Statistical Analysis

All continuous variables did not follow a Gaussian distribution in Kolmogorov-Smirnov test. Diffusion and perfusion parameters of the ischemic areas were compared with those of the control areas using Wilcoxon-signed rank test. The ratio of these parameters to the contralateral areas ([parameters of ischemic femoral head - parameters of control femoral head] / parameters of control femoral head) was compared among 4 different time points using Friedman test. Comparisons of ratios between two time points were performed using the Wilcoxon-signed rank sum test. Statistical significance was considered when *p* value was less than 0.05.

## RESULTS

### Radiographic and Histopathologic Assessment

Femoral heads with arterial deprivation revealed no demonstrable deformity such as sclerosis, fragmentation,



or collapse on plain radiographs (Fig. 2A). However, histopathologic changes were consistent with ischemic osteonecrosis in all involved femoral epiphysis at 2 weeks and 4 weeks after operation (70%, 7/10). No significant structural distortion was noted at 1 week after operation. Isolated bony trabeculae and empty lacunae were seen in the secondary ossification center. The surrounding growth plate showed decreased cellularity with an empty nest in the proliferative zone at 2 weeks after the operation (n = 4) (Fig. 2B-E). At 4 weeks after the operation, extensive intramedullary necrosis with collagen laying down was observed in the secondary ossification center and mild atrophy of the surrounding growth plate (n = 3).

### Diffusion MR Imaging

Apparent diffusion coefficient values in the secondary ossification center of the femoral head decreased in the ischemic hip during the immediate post-embolization period, rapidly increased during the 1-week postoperative period, and then maintained their levels until 4 weeks post-embolization compared to the control areas (Fig. 3A). ADC values of the control hips declined over time, which was consistent with previous reports (9). ADC values of

the ischemic hip did not show statistically significant ( $p = 0.189$ ) difference compared to those in the control hip (Table 1). The ADC ratio showed borderline significance ( $p = 0.086$ ) of time interval changes. The ADC ratios obtained immediately and 1 week post-embolization showed a statistically significant difference ( $p = 0.043$ ) (Table 2).

### Perfusion MR Imaging

A representative time-intensity curve of the proximal femoral epiphysis in the immediate postoperative period and 1 week after operation is shown in Figure 4. PE of the femoral epiphysis decreased immediately after embolization and then increased 1, 2, 4 weeks after the procedure. PE showed a statistically significant ( $p = 0.042$ ) difference compared to that of the control femoral head. TTP of the ischemic femoral head was delayed compared to that of the control areas ( $p = 0.048$ ). The  $V_e$  of the ischemic femoral head was significantly ( $p = 0.036$ ) higher than that of the control areas. Immediately after embolization,  $Wash_{out}$  was delayed and then recovered to a level similar to that of the control femoral head. The  $Kep$  was decreased immediately after embolization. It then became similar to that of the control femoral head (Table 1). Although

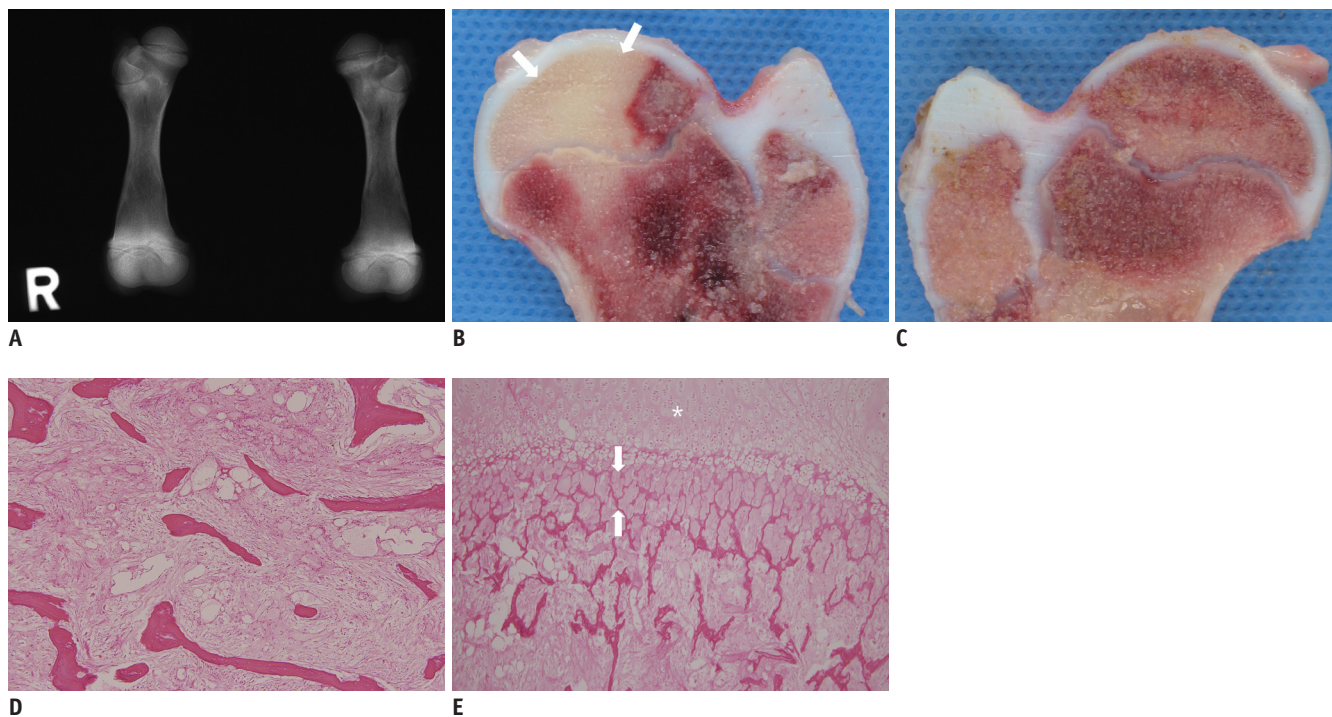


**Fig. 2. Gross and histopathologic findings at 2 weeks postoperative specimen.**

**A.** Faxitron radiography of harvested femurs showing no significant femoral head collapse or fragmentation. **B, C.** Gross cut section of ischemic area (**B**) demonstrating pale epiphyseal bone marrow (arrows) and metaphyseal congestion compared to contralateral areas (**C**). **D, E.** Microscopically, collagen fibers are seen in marrow cavity (**D**, hematoxylin and eosin stain, x 100). Note acellular zones (arrows, **E**) near growth plate (\*, **E**) (hematoxylin and eosin stain, x 40).

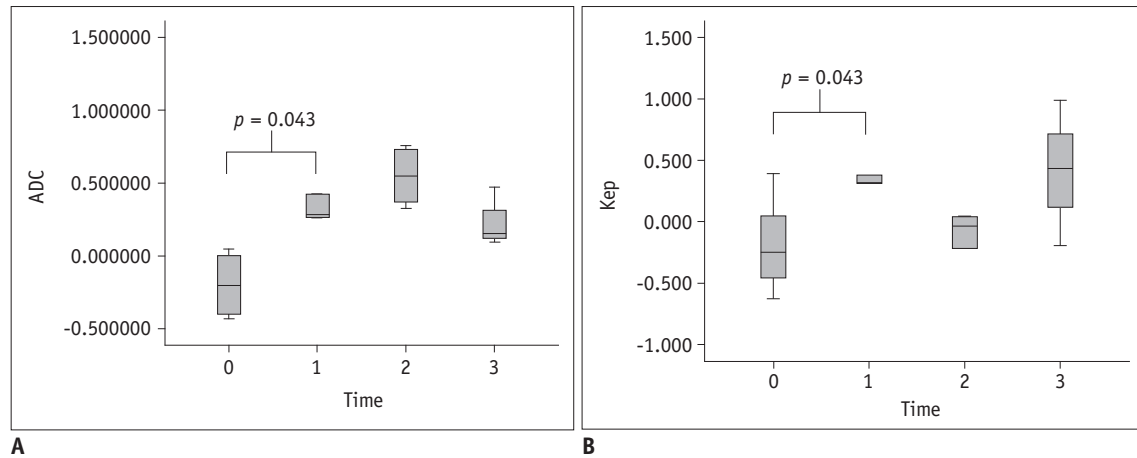


**Fig. 3. Time-interval change of diffusion and perfusion parameters.**

**A.** Relative ratio of ADC showing that ADC values in secondary ossification center of femoral head decreased in ischemic hip immediately after embolization, rapidly increased during 1-week postoperative period, and then maintained until 4 weeks post-embolization compared to control side. ADC ratios obtained immediately and 1 week post-embolization showed statistically significant difference ( $p = 0.043$ ). **B.** Kep ratio obtained immediately and 1 week post-embolization showed statistically significant difference ( $p = 0.043$ ). ADC = apparent diffusion coefficient

**Table 1. Comparison of Diffusion and Perfusion Parameters between Ischemic and Control Areas**

Parameters	Immediate	1 Week	2 Weeks	4 Weeks	$P^*$
ADC <sup>†</sup>					0.189
Ischemia	3.73 ± 1.39	4.54 ± 0.93	5.05 ± 2.10	3.76 ± 0.56	
Control	4.55 ± 0.93	3.56 ± 1.54	3.21 ± 1.09	3.13 ± 0.89	
PE					0.042
Ischemia	0.89 ± 0.54	1.43 ± 0.66	1.64 ± 0.77	0.52 ± 0.18	
Control	0.90 ± 0.56	1.08 ± 0.35	1.27 ± 0.71	0.43 ± 0.24	
TTP					0.048
Ischemia	1.37 ± 0.31	3.16 ± 3.55	2.75 ± 0.89	1.47 ± 0.61	
Control	1.19 ± 0.29	3.34 ± 4.24	2.20 ± 0.70	1.51 ± 0.79	
Wash <sub>out</sub>					0.626
Ischemia	1.54 ± 1.49	0.75 ± 0.10	1.25 ± 0.75	0.61 ± 0.06	
Control	0.89 ± 0.82	1.04 ± 0.17	1.10 ± 0.54	0.67 ± 0.07	
Kep					0.230
Ischemia	1.01 ± 0.57	0.98 ± 0.75	0.46 ± 0.46	0.85 ± 0.81	
Control	1.53 ± 1.15	0.93 ± 0.91	0.54 ± 0.47	0.89 ± 1.15	
Ve (unit)					0.036
Ischemia	1.02 ± 0.77	2.20 ± 2.52	1.95 ± 1.25	0.62 ± 0.06	
Control	0.86 ± 0.67	2.13 ± 2.66	1.53 ± 1.05	0.64 ± 0.07	

\*Wilcoxon signed rank test, <sup>†</sup>ADC ( $b = 700 \text{ s/mm}^2$ ) measurements are expressed as  $\times 10^{-4} \text{ mm}^2/\text{s}$ . ADC = apparent diffusion coefficient, EES = extravascular extracellular space, Kep = extraction rate between EES and vessels, PE = peak enhancement, TTP = time to peak, Ve = EES volume fraction, Wash<sub>out</sub> = wash-out parameter

changes in the perfusion ratio did not show statistically significant difference in the Friedman test, Kep values obtained immediately and 1 week post-embolization showed statistically significant ( $p = 0.043$ ) difference (Fig. 3B, Table 2).

## DISCUSSION

The hypotheses underlying this study were that arterial

deprivation could cause LCPD-like pathologic changes in the femoral head and that DCE-MRI could be used to detect changes in perfusion patterns in skeletally immature femoral head that is related functionally to bone and cartilage remodeling. Previous vascular deprivation-induced osteonecrosis of a rat model demonstrated loss of normal shape and height in femoral heads that mimicked LCPD. In addition, necrotic debris was seen substituted by fibrous tissue (5, 20). Kim et al. (6) also reported

**Table 2. Relative Ratio of Diffusion and Perfusion Parameters**

Ratio (Ischemia/Control)	Immediate	1 Week	2 Weeks	4 Weeks	P*
ADC	-0.19 ± 0.20	0.42 ± 0.47	0.55 ± 0.20	0.24 ± 0.20	0.086 <sup>†</sup>
PE	0.03 ± 0.15	0.28 ± 0.27	0.34 ± 0.32	0.28 ± 0.25	0.475
TTP	0.16 ± 0.17	0.05 ± 0.11	0.37 ± 0.32	0.01 ± 0.10	0.308
Wash <sub>out</sub>	1.05 ± 1.00	-0.26 ± 0.20	0.14 ± 0.40	-0.94 ± 0.01	0.615
Kep	-0.18 ± 0.34	0.28 ± 0.32	0.03 ± 0.70	0.41 ± 0.59	0.112 <sup>†</sup>
Ve	0.22 ± 0.30	0.11 ± 0.26	0.28 ± 0.46	-0.02 ± 0.03	0.896

\*Friedman test, <sup>†</sup>Wilcoxon signed rank test showed statistically significant difference between immediate postoperative period and 1 week ( $p = 0.043$ ). ADC = apparent diffusion coefficient, EES = extravascular extracellular space, Kep = extraction rate between EES and vessels, PE = peak enhancement, TTP = time to peak, Ve = EES volume fraction, Wash<sub>out</sub> = wash-out parameter

similar histopathologic changes in the femoral head due to ischemia in a piglet model of femoral neck ligation. They demonstrated femoral head flattening and fragmentation as well as histopathologic changes of the growth plate (6). Femoral neck ligation model of osteonecrosis is different from our model of arterial deprivation because it also causes venous obstruction, subsequently raising intraosseous pressure. We postulated that lack of gross deformity of the femoral head in our study might be related to the preservation of venous drainage and early reperfusion through collateral vessels.

During the immediate postoperative period, the signal intensity-time curve showed decreased PE, delayed TTP, and prolonged Wash<sub>out</sub> in the ischemic femoral heads. At that time, Kep as a rate constant between EES and blood plasma was decreased with restricted diffusion, suggesting that deprivation of the arterial supply could cause acute cellular swelling and restricted fluid shift from the EES into the intravascular extracellular space. At 1 week post embolization, PE increased with delayed TTP, suggesting spontaneous reperfusion through collateral channels. At that time, Kep of the ischemic femoral head became similar to that of the control femur with DWI showing increased diffusion, suggesting improved acute cellular swelling with increased intracellular water diffusivity and increased vascular permeability. At 2 weeks and 4 weeks after embolization, DWI showed persistently increased diffusion with high ADC compared to the corresponding values for the control femoral head. However, the perfusion parameter values became similar to those of the control femoral head at 2 to 4 weeks. These results are in consistent with those of previous studies (9, 10). Yoo et al. (10) mentioned that DWI imaging had a potential prognostic value in a patient with LCPD. Menezes et al. (9) reported that the diffusion changes may be a better indicator of femoral head damage than enhancement changes that may precede gross

deformity.

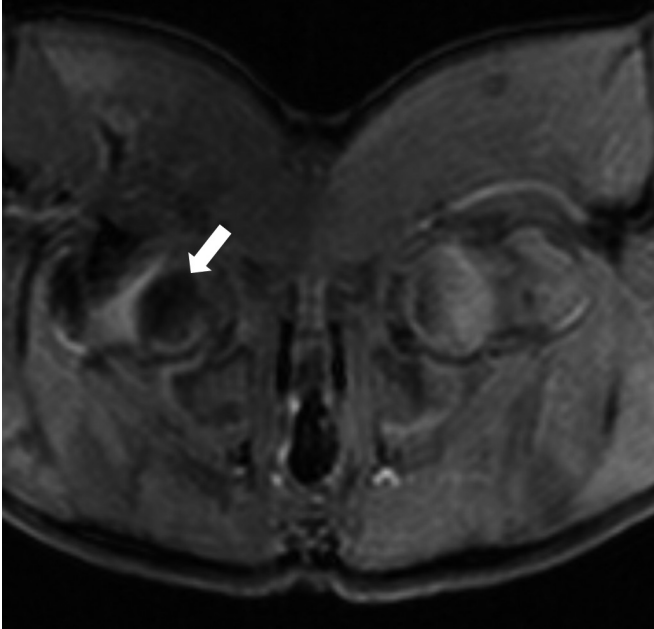
In contrast to conventional contrast-enhanced MRI which simply displays contrast enhancement at a single point in time, DCE-MRI provides pharmacokinetic information. DCE-MRI is based on the acquisition of serial T1-weighted images before, during, and after administration of a gadolinium-based contrast agent. The resulting signal intensity-time curve can be used to extract quantitative information concerning fluid kinetics (21, 22). Contrast enhancement is linearly correlated to the concentration of the contrast materials in both blood and tissue. Blood flow can be estimated from the transit time of the contrast materials. Because signal enhancement is related to the perfusion of contrast materials and the blood flow, changes in tissue perfusion can be inferred from the signal intensity-time curves (23). Prolonged signal enhancement in the outflow phase has been associated with venous outflow obstruction, stasis, and decreased perfusion. Our signal intensity-time curves showed clear and significant differences in the outflow phase of contrast administration. Inflow parameters (slope and amplitude) changed, indicating that the delivery of contrast materials to the femoral epiphysis was disturbed. The outflow parameters including wash-out were significantly changed as evidenced by the difference in the slope of the outflow or wash-out phase on the signal intensity-time curves (24, 25). The intraosseous extravascular extracellular compartment of the immature femoral epiphysis is complex. It is comprised of several tissues, predominantly fat, hematopoietic bone marrow, compact bone, and cartilage. Gadolinium does not have access to all these compartments. The Ve (volume of the extravascular compartment) and Kep (a rate constant between EES and blood plasma) can be estimated from the pharmacokinetic model. These parameters are related to vascular permeability.

There are several limitations of our study. First, the

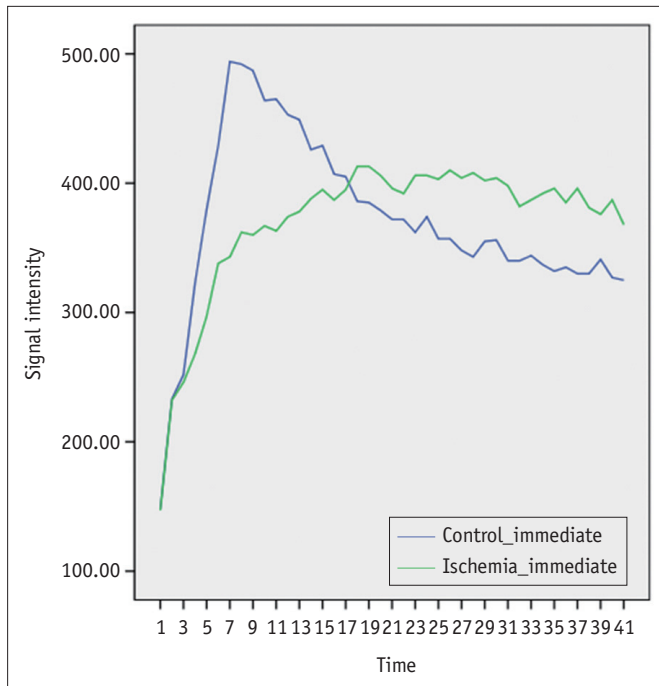
Effect of Arterial Deprivation on Growing Femoral Epiphysis

number of experimental models was too small to achieve a strong statistical power in DWI and DCE-MRI variable as well as pathologic findings. Thus, a larger-scale study may reveal that those variables found to be insignificant

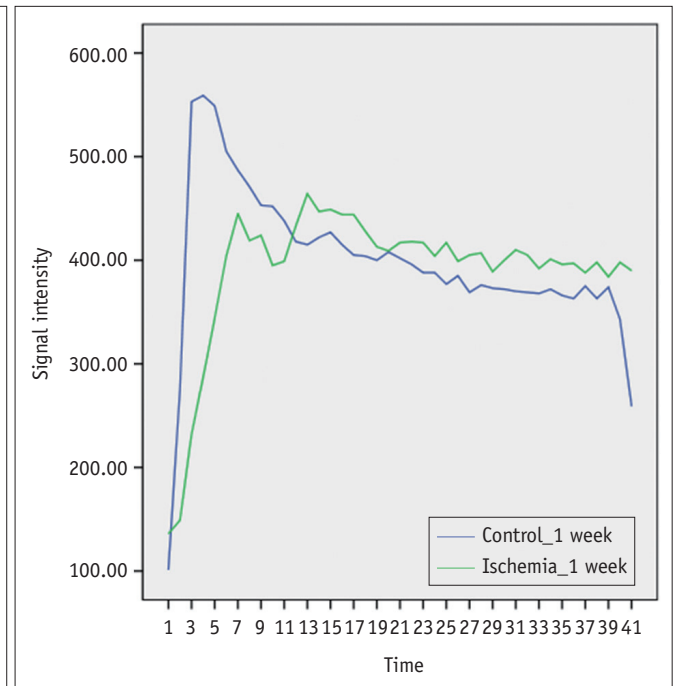
in our study might be significant. Secondly, we could not reproduce an experimental model of LCPD that manifests fragmentation and collapse of the femoral head. A piglet model of a femoral neck ligation is a well-established model



A



B



C

**Fig. 4. Signal intensity-time curves.**

**A.** Dynamic contrast enhanced T1-weighted image obtained immediately after embolization demonstrating markedly decreased contrast enhancement in right femoral head (arrow). **B.** Signal intensity-time curve obtained in immediate postoperative period demonstrating decreased peak enhancement, delayed time-to-peak, and persistent enhancement on wash-out phase in ischemic area. **C.** Signal intensity-time curve of same experimental animal obtained 1 week after embolization showing shortened time-to-peak and partially improved delayed wash-out in ischemic area.



of the femoral head ischemia that mimics LCPD in children. In that model, both arterial and venous obstructions are induced through surgical exposure of the proximal femur and subsequent ligation of the whole vessels around the femoral neck. Our study was planned to evaluate early ischemic change of the femoral head using DCE-MRI and DWI. Therefore, we chose an arterial occlusion model rather than a surgical ligation model to avoid surgical artifacts on MR imaging. In our study, femoral-head fragmentation and collapse were not seen on plain radiographs, although ischemic tissue damage could be observed on pathologic specimens. Subsequent establishment of collateral circulation after occlusion of the medial femoral circumflex artery might prevent extensive necrosis or collapse of the femoral epiphysis. Another explanation would be that venous obstruction may be more important than arterial occlusion or at least have an additive effect to the arterial occlusion in the development of osteonecrosis in the immature femoral head. Thirdly, there was a technical limitation of contrast infusion. We did not use an automatic power injector due to the fragility of the vessels in the piglet, which might have limited the interpretation of pharmacokinetics in our experimental model.

In summary, an arterial occlusion model of femoral head ischemia induced ischemic tissue damage in the femoral head of immature piglets. Diffusion decreased immediately after ischemic insult, but soon increased and maintained a high level even after reperfusion developed. Vascular permeability increased early and spontaneous reperfusion of the femoral head occurred in the event of arterial deprivation. Therefore, diffusion MRI and a pharmacokinetic model obtained from the DCE-MRI data are useful in depicting early changes of perfusion and tissue damage in the model of femoral head ischemia in skeletally immature piglets.

## REFERENCES

- Kim HK, Herring JA. Pathophysiology, classifications, and natural history of Perthes disease. *Orthop Clin North Am* 2011;42:285-295, v
- Kim HK. Pathophysiology and new strategies for the treatment of Legg-Calvé-Perthes disease. *J Bone Joint Surg Am* 2012;94:659-669
- Boss JH, Misselevich I. Osteonecrosis of the femoral head of laboratory animals: the lessons learned from a comparative study of osteonecrosis in man and experimental animals. *Vet Pathol* 2003;40:345-354
- Alpaslan AM, Aksoy MC, Yazici M. Interruption of the blood supply of femoral head: an experimental study on the pathogenesis of Legg-Calvé-Perthes Disease. *Arch Orthop Trauma Surg* 2007;127:485-491
- Norman D, Reis D, Zinman C, Misselevich I, Boss JH. Vascular deprivation-induced necrosis of the femoral head of the rat. An experimental model of avascular osteonecrosis in the skeletally immature individual or Legg-Perthes disease. *Int J Exp Pathol* 1998;79:173-181
- Kim HK, Stephenson N, Garces A, Aya-ay J, Bian H. Effects of disruption of epiphyseal vasculature on the proximal femoral growth plate. *J Bone Joint Surg Am* 2009;91:1149-1158
- Li X, Qi J, Xia L, Yu C, Peng W, Hu X, et al. Dynamic gadolinium-enhanced MRI in early ischaemia of the proximal femoral epiphysis--a preliminary study. *Clin Radiol* 2008;63:1149-1159
- Tsao AK, Dias LS, Conway JJ, Straka P. The prognostic value and significance of serial bone scintigraphy in Legg-Calvé-Perthes disease. *J Pediatr Orthop* 1997;17:230-239
- Menezes NM, Connolly SA, Shapiro F, Olear EA, Jimenez RM, Zurakowski D, et al. Early ischemia in growing piglet skeleton: MR diffusion and perfusion imaging. *Radiology* 2007;242:129-136
- Yoo WJ, Kim YJ, Menezes NM, Cheon JE, Jaramillo D. Diffusion-weighted MRI reveals epiphyseal and metaphyseal abnormalities in Legg-Calvé-Perthes disease: a pilot study. *Clin Orthop Relat Res* 2011;469:2881-2888
- Sebag G, Ducou Le Pointe H, Klein I, Maiza D, Mazda K, Bensahel H, et al. Dynamic gadolinium-enhanced subtraction MR imaging--a simple technique for the early diagnosis of Legg-Calvé-Perthes disease: preliminary results. *Pediatr Radiol* 1997;27:216-220
- Lamer S, Dorgeret S, Khairouni A, Mazda K, Brillet PY, Bacheville E, et al. Femoral head vascularisation in Legg-Calvé-Perthes disease: comparison of dynamic gadolinium-enhanced subtraction MRI with bone scintigraphy. *Pediatr Radiol* 2002;32:580-585
- Courcoutsakis N, Spanoudaki A, Maris TG, Astrinakis E, Spanoudakis E, Tsatalas C, et al. Perfusion parameters analysis of the vertebral bone marrow in patients with Ph<sup>1-</sup> chronic myeloproliferative neoplasms (Ph(neg) MPN): a dynamic contrast-enhanced MRI (DCE-MRI) study. *J Magn Reson Imaging* 2012;35:696-702
- De Coninck T, Jans L, Sys G, Huysse W, Verstraeten T, Forsyth R, et al. Dynamic contrast-enhanced MR imaging for differentiation between enchondroma and chondrosarcoma. *Eur Radiol* 2013;23:3140-3152
- Lecouvet FE, Larbi A, Pasoglou V, Omoumi P, Tombal B, Michoux N, et al. MRI for response assessment in metastatic bone disease. *Eur Radiol* 2013;23:1986-1997
- Boesen M, Kubassova O, Bouert R, Axelsen MB, Ostergaard M, Cimmino MA, et al. Correlation between computer-aided dynamic gadolinium-enhanced MRI assessment of inflammation and semi-quantitative synovitis and bone marrow oedema scores of the wrist in patients with



- rheumatoid arthritis--a cohort study. *Rheumatology (Oxford)* 2012;51:134-143
17. Griffith JF, Yeung DK, Leung JC, Kwok TC, Leung PC. Prediction of bone loss in elderly female subjects by MR perfusion imaging and spectroscopy. *Eur Radiol* 2011;21:1160-1169
  18. Budzik JF, Lefebvre G, Forzy G, El Rafei M, Chechin D, Cotten A. Study of proximal femoral bone perfusion with 3D T1 dynamic contrast-enhanced MRI: a feasibility study. *Eur Radiol* 2014;24:3217-3223
  19. Chan WP, Liu YJ, Huang GS, Lin MF, Huang S, Chang YC, et al. Relationship of idiopathic osteonecrosis of the femoral head to perfusion changes in the proximal femur by dynamic contrast-enhanced MRI. *AJR Am J Roentgenol* 2011;196:637-643
  20. Sabo E, Peskin B, Misselevich I, Zinman C, Levin D, Norman D, et al. Computer-assisted image analysis of the rat postosteonecrotic remodeled femoral head. *Exp Mol Pathol* 2001;71:256-264
  21. Ferré JC, Shiroishi MS, Law M. Advanced techniques using contrast media in neuroimaging. *Magn Reson Imaging Clin N Am* 2012;20:699-713
  22. Choi HS, Kim AH, Ahn SS, Shin NY, Kim J, Lee SK. Glioma grading capability: comparisons among parameters from dynamic contrast-enhanced MRI and ADC value on DWI. *Korean J Radiol* 2013;14:487-492
  23. Law M, Young R, Babb J, Rad M, Sasaki T, Zagzag D, et al. Comparing perfusion metrics obtained from a single compartment versus pharmacokinetic modeling methods using dynamic susceptibility contrast-enhanced perfusion MR imaging with glioma grade. *AJNR Am J Neuroradiol* 2006;27:1975-1982
  24. Brix G, Semmler W, Port R, Schad LR, Layer G, Lorenz WJ. Pharmacokinetic parameters in CNS Gd-DTPA enhanced MR imaging. *J Comput Assist Tomogr* 1991;15:621-628
  25. Tofts PS, Kermode AG. Measurement of the blood-brain barrier permeability and leakage space using dynamic MR imaging. 1. Fundamental concepts. *Magn Reson Med* 1991;17:357-367